

VILNIUS UNIVERSITY
CENTER FOR PHYSICAL SCIENCES AND TECHNOLOGY
INSTITUTE OF PHYSICS

AIDAS ALEKNAVIČIUS

INVESTIGATION OF COMPOSITE LASER ACTIVE ELEMENTS WITH
THIN DOPED LAYERS

Summary of doctoral dissertation
Technology sciences, material engineering (08 T)

Vilnius, 2013

Doctoral dissertation was prepared during 2008-2012 at Institute of Physics of the Center for Physical Sciences and Technology.

Scientific supervisor:

dr. **Andrejus Michailovas** (Center for Physical Sciences and Technology, technology sciences, material engineering – 08 T).

Doctoral dissertation will be defended in the Council of Material engineering of Vilnius University:

Chairman: prof. habil. dr. **Valerijus Smilgevičius** (Vilnius University, Technology sciences, material engineering – 08 T).

Members:

dr. **Raimondas Petruškevičius** (Center for Physical Sciences and Technology, Technology sciences, material engineering – 08 T);

prof. habil. dr. **Eugenijus Šatkovskis** (Vilnius Gediminas Technical University, Technology sciences, material engineering – 08 T);

dr. **Rimantas Grigonis** (Vilnius University, Technology sciences, material engineering – 08 T);

dr. **Asta Guobienė** (Kaunas University of Technology, Technology sciences, material engineering – 08 T).

Opponents:

dr. **Virgilijus Vaičaitis** (Vilnius University, Technology sciences, material engineering – 08 T)

dr. **Audrius Pugžlys** (Vienna University of Technology, Technology sciences, material engineering – 08 T)

The thesis will be under open consideration on the 18th of September, 2013 3p.m. at the hall of Institute of physics, Center for Physical Sciences and Technology, Savanoriu ave. 231, LT-02300, Vilnius, Lithuania.

Summary of dissertation was distributed on August 14th, 2013.

Dissertation is available at libraries of Vilnius University and Center for Physical Sciences and Technology.

VILNIAUS UNIVERSITETAS
FIZINIŲ IR TECHNOLOGIJOS MOKSLŲ CENTRAS
FIZIKOS INSTITUTAS

AIDAS ALEKNAVIČIUS

SUDĖTINIŲ AKTYVIŲ LAZERINIŲ ELEMENTŲ SU PLONAIŠ
LEGIRUOTAIS SLUOKSNIAIS TYRIMAS

Daktaro disertacijos santrauka
Technologijos mokslai, medžiagų inžinerija (08 T)

Vilnius, 2013

Daktaro disertacija rengta 2008-2012 metais Fizinių ir technologijos mokslų centre, Fizikos institute.

Darbo vadovas:

dr. **Andrejus Michailovas** (Fizinių ir technologijos mokslų centras, technologijos mokslai, medžiagų inžinerija – 08 T).

Disertacija ginama Vilniaus universiteto Technologijos mokslo krypties taryboje:

Pirmininkas: prof. habil. dr. **Valerijus Smilgevičius** (Vilniaus Universitetas, technologijos mokslai, medžiagų inžinerija – 08 T).

Nariai:

dr. **Raimondas Petruškevičius** (Fizinių ir technologijos mokslų centras, technologijos mokslai, medžiagų inžinerija – 08 T);

prof. habil. dr. **Eugenijus Šatkovskis** (Vilniaus Gedimino Technikos Universitetas, technologijos mokslai, medžiagų inžinerija – 08 T);

dr. **Rimantas Grigonis** (Vilniaus Universitetas, technologijos mokslai, medžiagų inžinerija – 08 T);

dr. **Asta Guobienė** (Kauno Technologijos Universitetas, technologijos mokslai, medžiagų inžinerija – 08 T).

Oponentai:

dr. **Virgilijus Vaičaitis** (Vilniaus Universitetas, technologijos mokslai, medžiagų inžinerija – 08 T)

dr. **Audrius Pugžlys** (Vienos Technikos Universitetas, technologijos mokslai, medžiagų inžinerija – 08 T)

Disertacija bus ginama viešame Technologijos mokslo krypties tarybos posėdyje 2013 m. rugsėjo mėn. 18 d. 15 val. Fizinių ir technologijos mokslų centre, Fizikos instituto salėje.

Adresas: Savanorių pr. 231, LT-02300, Vilnius, Lietuva.

Disertacijos santrauka išsiuntinėta 2013 m. rugpjūčio mėn. 14 d.

Disertaciją galima peržiūrėti Vilniaus universiteto ir Fizinių ir technologijos mokslų centro bibliotekose.

Table of contents

Introduction	7
Main objectives and tasks	7
Novelty of this work.....	8
Statements to be defended.....	8
Approbation.....	9
Publications	9
Presentations at conferences.....	9
Author's contributions.....	11
Contribution of co-authors	11
1 Commonly used types of solid state laser elements. Concept of multi-disk laser element.....	12
2 Theoretical models and principals of calculations	14
2.1 Composite multi-disk laser element	14
2.2 Propagation of pump beam.....	16
2.3 Nd:YAG absorption, amplification, heat generation.....	17
2.4 Calculation of heat flows and deformations	19
2.5 Optical aberrations.....	20
2.6 Method for evaluation of aberrations	21
2.7 Calculation of laser beam parameters.....	22
3 Experiments	23
3.1 Composite element	23
3.2 Experimental validation of theoretical models.....	26
4 Theoretical estimation of optical properties of composite active elements	30
4.1 Model geometry.....	31
4.2 Evaluation of influence of undoped layer.....	32

4.3 Estimations for alternative multi-disk configuration.....	36
Conclusions	37
References	38
Santrauka	40
Brief information about the author	41

Introduction

Demands on nano- or pico-second high-power and high beam quality lasers are increasing recently in the areas of electronics and microfabrication. High beam quality is demanded as it allows radiation to be focused to a smaller spot, thus increasing a precision of fabrication. Such lasers are capable to perform various technological operations. A smart-phone iPhone can be taken as an example, where precise treatment is required and some parts were manufactured employing lasers.

Main limiting factors for high power high brightness beam generation are related to thermal effects emerging from heat generated in active medium. Various configurations of active elements were developed to have advantages in specific areas. Unfortunately, improvements in one area usually mean exacerbation in other areas. As an example, rod type active elements are capable to generate or amplify high energy pulses, but average power is limited if high quality beam is demanded. Fiber lasers can generate high power diffraction limited laser beams, but are limited by a peak intensity of a pulse. Disk lasers provide high power, high quality laser beams, but are not handy to generate high energy pulses.

Active laser element which combines decent properties of various laser elements was proposed in this work.

Main objectives and tasks

- To analyze and elaborate a concept of composite laser element and its application possibilities.
- To investigate generation and amplification properties of proposed active laser element experimentally.
- To develop theoretical models describing optical properties of proposed laser element.
- To confirm developed models experimentally.
- To find factors limiting applicability of proposed laser element.

Novelty of this work

- The use of composite materials expands technological possibilities in various areas. Laser technologies are not exceptions. Improvements in manufacturing of transparent ceramics allow producing high quality laser elements of custom shape, size and composition. This area is still not investigated widely.
- A laser element of novel type was introduced in this work, expecting it to enable of producing high quality laser beam with a power of more than 50 watts. Realization of such laser would increase competitive ability of Lithuanian lasers in global market, especially in industrial area.
- By the use of experimentally confirmed theoretical models, thermo-optical properties of thin active disk with undoped layer on top, was investigated. Influence of undoped layer on thin active disk was not investigated till now.
- Additionally, an original method to rate induced optical aberrations which allows unambiguous comparison of different aberrations was presented. Further development of this method has a potential to be applied in designing and analysis of laser systems.

Statements to be defended

1. Geometry of slab shaped composite laser active element was presented and elaborated. Experimental results show that this solution does not have an advantage over common rod type laser elements despite its similarity to thin-disk laser elements, which are characterized to have low thermally induced aberrations.
2. A method to rate different optical phase distortions by calculating resulting M^2 parameter of an affected diffraction limited laser beam was proposed. This method allows an unambiguous comparison of optical aberrations induced by different optical elements if a size of initial probing Gaussian beam is defined. This method allows an evaluation of tolerance of laser element to a heat-load.
3. Introducing undoped layer on top of thin active layer changes heat flow and temperature distribution in the way that additional detrimental aberrations are induced which deteriorates characteristics (M^2) of reflected laser beam.

Approbation

Publications

A. Aleknavičius, R. Smilingis, M. Grishin, A. Michailovas, K. Michailovas, J. Pilipavičius, V. Girdauskas, M. Gabalis, Concept and realization of collinearly pumped multiple thin disk active medium, *Quantum Electronics* **41** (7) 590 -594 (2011).

A. Aleknavičius, M. Gabalis, A. Michailovas, V. Girdauskas, Aberrations induced by anti-ASE cap on thin-disk active element, *Optics Express* **21** (12) 14530-14538 (2013).

Presentations at conferences

1. **A. Aleknavičius**, R. Smilingis, Multidiskinio lazerinio stiprintuvo koncepcijos tyrimai, 38-oji Lietuvos nacionalinė konferencija LNFK38, Vilnius, Lietuva, 2009.
2. **A. Aleknavičius**, R. Smilingis, Light amplification by thin active medium, XVIII Lithuanian –Belarussian seminar “Lasers and Optical Nonlinearity”, Vilnius, Lietuva, 2009.
3. **A. Aleknavičius**, R. Smilingis, M. Grishin, A. Michailovas, J. Pilipavičius, Concept of collinearly pumped multiple thin disk active medium, 14th conference on laser optics, St.Petersburg, Russia, 2010 m.
4. **A. Aleknavičius**, R. Smilingis, M. Grishin, A. Michailovas, J. Pilipavičius, Concept of collinearly pumped multiple thin disk active medium, A. von Humboldt forumas 'Mokslas ir visuomenė moderniojoje Europoje', Vilnius, Lietuva, 2010.
5. **A. Aleknavičius**, R. Smilingis, M. Grishin, A. Michailovas, K. Michailovas, J. Pilipavičius, V. Girdauskas, Kolineariai kaupinamos daugiadiskines aktyviosios terpes koncepcija, 1-oji FTMC doktorantu ir jaunuju mokslininku konferencija FizTeCh2010, Vilnius, Lietuva, 2010.
6. **A. Aleknavičius**, R. Smilingis, M. Grishin, A. Michailovas, K. Michailovas, J. Pilipavičius, V. Girdauskas, Concept and realization of collinearly pumped multiple thin disk active medium, Advanced Solid-State Photonics (ASSP) conference, Istanbul, Turkey, 2011.

7. M. Gabalis, V. Girდაuskas, **A. Aleknavičius**, A. Michailovas, D. Jokšas, Numerical simulation of cooling of thin active laser elements, XIX Belarusian-Lithuanian seminar „Lasers and optical nonlinearity“, Minsk, Belarus, 2011.
8. M. Gabalis, V. Girდაuskas, **A. Aleknavičius**, A. Michailovas, Numerical Simulation of Thermal Effects in Composite Nd:YAG Slab Laser Active Medium With Collinear Zig-zag Pumping, Conference on Lasers and Electro-Optics (CLEO Europe), Munich, Germany, 2011.
9. **A. Aleknavičius**, A. Michailovas, M. Gabalis, V. Girდაuskas, Optical properties of composite Nd:YAG ceramic slab laser active element with collinear zig-zag pumping, 2nd EOS Topical Meeting on Lasers (ETML'11) Capri, Italy, 2011.
10. **A. Aleknavičius**, K. Michailovas, A. Michailovas, M. Gabalis, V. Girდაuskas, Kolineariai žadinamo kompozitinio keraminio Nd:YAG aktyviojo lazerinio elemento stiprinimo matavimai, 2-oji FTMC doktorantu ir jaunųjų mokslininkų konferencija FizTeCh2011, Vilnius, Lietuva, 2011.
11. M. Gabalis, **A. Aleknavičius**, A. Budinavičius, V. Girდაuskas, Plokščio kompozitinio kolineariai zigzagu kaupinamo ND:YAG lazerio šiluminių savybių skaitinis modeliavimas, 39-oji Lietuvos nacionalinė konferencija LNFK39, Vilnius, Lietuva, 2011
12. **A. Aleknavičius**, K. Michailovas, A. Michailovas, M. Gabalis, V. Girდაuskas, Kolineariai žadinamo kompozitinio keraminio Nd:YAG aktyviojo lazerinio elemento stiprinimo matavimai, 39-oji Lietuvos nacionalinė konferencija LNFK39, Vilnius, Lietuva, 2011.
13. **A. Aleknavičius**, M. Gabalis, A. Michailovas, M. Grishin, K. Michailovas, V. Girდაuskas, Gain measurements of composite Nd:YAG ceramic slab laser active element with collinear zig-zag pumping, Advanced Solid-State Photonics (ASSP) conference, San Diego, USA, 2012.
14. **A. Aleknavičius**, M. Gabalis, A. Michailovas, M. Grishin, V. Girდაuskas, Measurements of optical aberrations in zig-zag pumped composite slab, 15th conference on laser optics, St.Petersburg, Russia, 2012.

Author's contributions

Elaboration of the concept of composite active element.

Designing, measuring and analyzing data of experiments.

Development of theoretical models, optimization of calculation methods, calculations.

Designing, performing and development of experiments for confirming of theoretical models.

Creation, development and application of an original method to rate aberrations.

Interpretation of obtained results. Preparation for publications.

Composing of publications and presentations in conferences.

Contribution of co-authors

Dr. Mikhail Grishin proposed a concept of composite active element (patent pending).

Martynas Gabalis and dr. Valdas Girdauskas performed calculation using Comsol Multiphysics® software according to formulated tasks.

Supervisor Andrejus Michailovas was consulting throughout whole process of work.

1 Commonly used types of solid state laser elements. Concept of multi-disk laser element

In this section properties of common types of geometries of laser elements are briefly overviewed. Main advantages and disadvantages are presented together with main limiting factors for obtaining desired laser beam parameters. This overview is confined to generation of high power diffraction limited laser beams by active elements pumped by laser diodes (LD) excluding such pumping systems as flash lamps. Types of elements under discussion in dissertation are: fibers, rods, slabs and thin-disks.

Finally, a concept of a composite laser element with thin active layers is introduced which combines positive properties of thin-disk, SLAB and rod laser elements avoiding their negative properties.

According to its properties, a proposed element is mostly similar to a thin-disk active laser element. In essence, it is a structure of several thin-disk elements (Fig. 1.1). Compared to a single thin-disk, such structure has a higher absorption of pump radiation and higher gain for laser radiation. In presence of the same total absorbed pump power, heat is distributed between each disk. Amplified spontaneous emission (ASE) is reduced also as excitation density decreases.

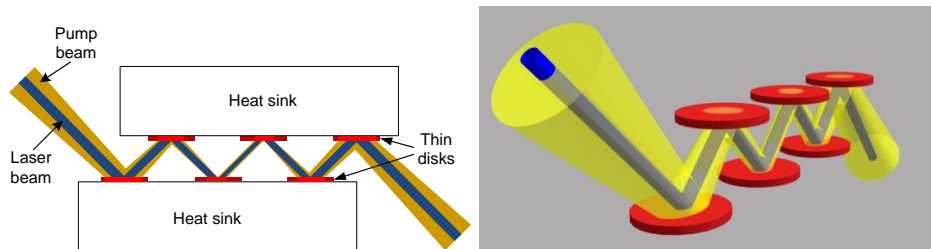


Fig. 1.1 Schematic view of multiple-disk structure

Pumping scheme of such structure should be collinear to generated beam as it is realized in end-pumped laser rods. This approach provides effective use of pump power. Pump beam does not necessarily have to be size-matched to laser beam, but lower diffraction of pump beam result in power efficiency of the system.

Amount of thin-disks is related to several factors. Using more disks would result in higher absorption, amplification and energy storage. But it would make structure bigger and higher demands on pump beam properties would be required. Absorbed power variation between individual disks would also be larger.

By filling the air-gap between two planes of thin-disks (Fig. 1.1) with undoped medium we would obtain similar element (Fig. 1.2). Such element can be made like one monolithic composite element where only thin side layers are doped (Fig. 1.2). In comparison to “separate thin-disk” structure, the filling of undoped medium provides some advantages which are described with more details in dissertation.

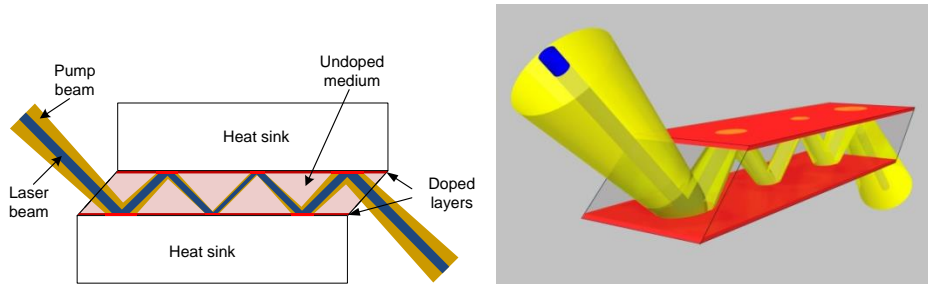


Fig. 1.2 Schematic view of composite active element with thin active layers.

In principle, monolithic design reduces requirements for pump beam, total internal reflection can be employed, higher absorption can be achieved and such element is easier to handle. ASE is also suppressed due to undoped medium [1]. ASE suppression was demonstrated in [2].

It is also expected that thermally induced aberration should be drastically reduced by the presence of undoped layer [3]. But it is worth to note that results in [3] conflicts with results in [2].

Possibility of realization of such element is related to the successful development of transparent ceramics manufacturing technologies which already allow producing a high quality laser element with a desired shape and composition [4]. The lack of acceptable technology for ceramics may be the answer why such elements were not been tested earlier.

Main drawback of proposed element is the price.

Even if ytterbium is commonly used in thin-disk lasers as active ions, we chose to use neodymium instead. It was shown, that neodymium ions have potential in thin-disk lasers as well [5].

According to achievements in thin-disk laser area it was expected to obtain a diffraction-limited laser beams with the power levels over 50W by using proposed laser element.

2 Theoretical models and principals of calculations

In this section geometrical parameters and optical properties are estimated for the proposed composite element. Then theoretical models which are used in further calculations are presented. Some specifics of calculations in discrete case are presented also.

2.1 Composite multi-disk laser element

2.1.1 Geometry

The geometry of element is defined by several aspects which were described in dissertation. Drawing of the resulting element which was later manufactured for experiments is shown in Fig. 2.1. The angle of incidence θ was defined by conditions of total internal reflection keeping in mind that pump beam also has its angular distribution. As a protective layer of SiO_2 was deposited on the element, the angle of incidence was chosen to be $\theta = 62^\circ$. Number of active zones was 6. Height of the element was $h = 2.5\text{mm}$ and resulting length was $l = 29.5\text{mm}$.

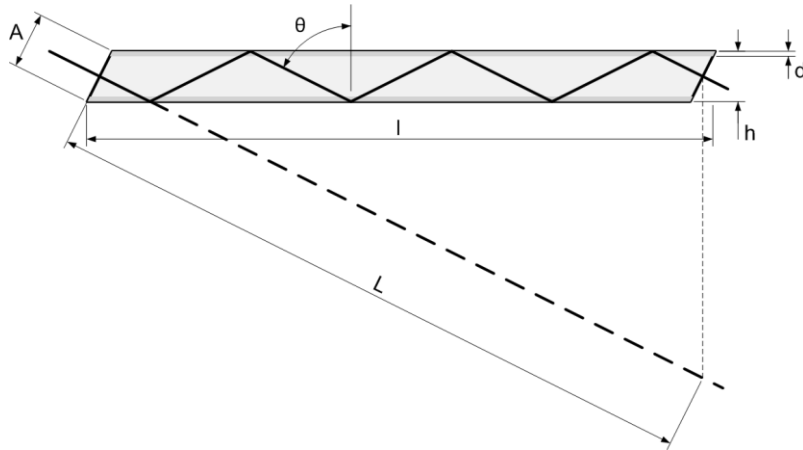


Fig. 2.1 Geometry parameters of composite element.

Thickness of active layers was 0.2 mm with Nd^{3+} doping concentration of 2 at %. More details are presented in dissertation.

2.1.2 Estimation of optical properties

Several collinear pump schemes are analyzed in dissertation. Each option is analyzed in respect of absorbed power distribution and optimal absorption parameters are evaluated. It was estimated, that optimal absorption of thin doped layer after one

“bounce” is about 29% when pumping is organized from both sides without returning unabsorbed pump radiation.

In case of total internal reflection (TIR), the phase of reflected wave change. Estimated phase difference between p and s polarizations for element used in experiments is $\Delta\phi \approx 0.72\pi = 0.36\lambda$. Such kind of wave-plate property sometimes may be an issue and it was concluded in dissertation that, there’s a need to pay attention to polarization when laser elements employing TIR are used.

In order to evaluate induced optical aberrations by laser element due to thermal effects, there’s a need to evaluate temperature distribution inside the element and deformations of reflecting surfaces due to thermal expansion. The finite element analysis software Comsol Multiphysics was used for this modeling. Power of pump beam was set to be 100 W (50 W from each side). On behalf of simplicity it was assumed that pump beam diameter (1.5 mm) is the same across the whole length of element having top-hat intensity distribution. Absorbed pump power conversion to heat was set to be 30%. Distribution of absorbed power between active zones was set to be according to optimized absorption of single active area. Thickness of doped layer where heat is generated was $d = 200 \mu m$ (Fig. Fig. 2.1). Heat was set to flow to copper heat-sink through a $100 \mu m$ thick indium bonding layer. Back side temperature of copper heat-sinks was fixed to $T_0 = 16^\circ C$. All material parameters were set to be used from Comsol Multiphysics data-base. Heat flows through interfaces were set to be ideal (continuity).

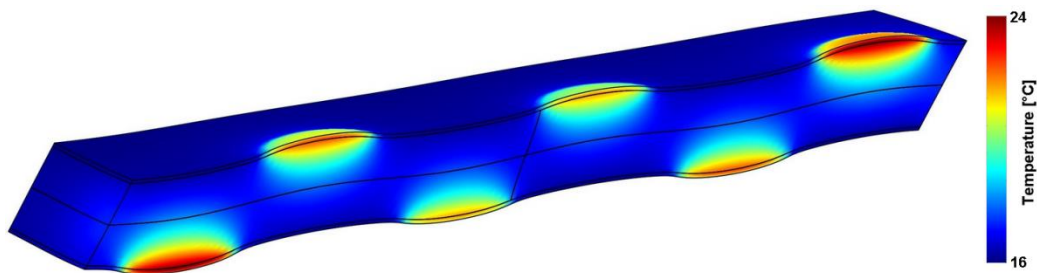


Fig. 2.2 Calculated distributions of temperature and deformations by simplified numerical model (deformations magnified by a factor of 4000)

Results of calculations are presented in Fig. 2.2. Results show that maximum temperature rise was 8 K and deformations were less than 100 nm. Thus even if we could predict thermal-lensing effect, it seemed to be negligible.

2.2 Propagation of pump beam

Usually the coherence length of a pump radiation is short, thus beam propagation may be described by the use of geometric optics, namely matrices. Even if ray propagation angle to optical axis may be large, matrix method can still be used when angles are replaced by tangents of those angles.

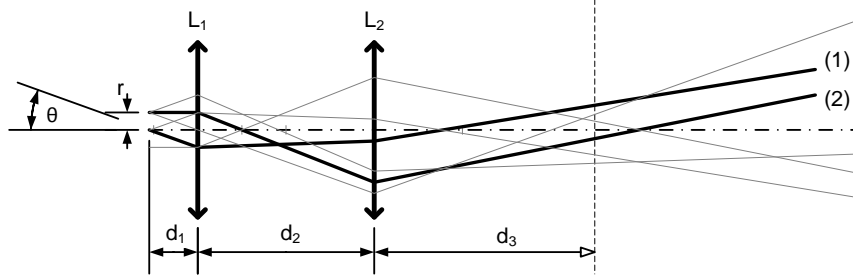


Fig. 2.3 Schematic view of pump formation optical system.

Schematic view of optical system consisting of two lenses is shown in Fig. 2.3. The matrix of such system is as follows:

$$\begin{bmatrix} r_{out} \\ \theta_{out} \end{bmatrix} = \begin{bmatrix} 1 & d_3 \\ 0 & 1 \end{bmatrix} \begin{bmatrix} 1 & 0 \\ -D_2 & 1 \end{bmatrix} \begin{bmatrix} 1 & d_2 \\ 0 & 1 \end{bmatrix} \begin{bmatrix} 1 & 0 \\ -D_1 & 1 \end{bmatrix} \begin{bmatrix} 1 & d_1 \\ 0 & 1 \end{bmatrix} \begin{bmatrix} r_{in} \\ \theta_{in} \end{bmatrix}. \quad (2.1)$$

This equation can be used to find the position of a ray at certain distance from the last lens when position and angle at the fiber-end is defined:

$$\begin{aligned} r_{out} = & [1 - d_3 D_2 - ((1 - d_3 D_2) d_2 + d_3) D_1] r_{in} + \\ & + [(1 - d_3 D_2 - ((1 - d_3 D_2) d_2 + d_3) D_1) d_1 + \\ & + (1 - d_3 D_2) d_2 + d_3] \theta_{in} \end{aligned} \quad (2.2)$$

This equation can be written in such form:

$$r_{out} = k_r(d_3) \cdot r_{in} + k_\theta(d_3) \cdot \theta_{in}. \quad (2.3)$$

An assumption was made that angular spectrum of the emerging beam is the same for every point on end-surface of fiber. Then it is shown that intensity distribution of pump beam is a convolution of two scaled functions which are lateral and angular intensity distributions at fiber end:

$$I_{d_3}(r) = f(k_r r) * g(k_\theta \theta) \quad (2.4)$$

This simple model can be used to show that pump beam can be asymmetric in respect of its waist. It is also powerful enough to be used in simulation of a real fiber coupled pump beam as it was manifested by good agreement of calculated and measured data.

2.3 Nd:YAG absorption, amplification, heat generation

Nd:YAG medium is often described as a four energy level system. Nevertheless, it has a quite complex energy level system which sometimes may be necessary to pay attention to (Fig. 2.4) [6].

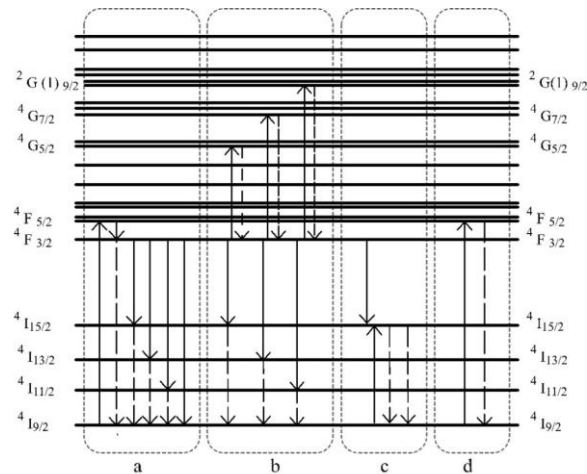


Fig. 2.4 Energy level structure of Nd:YAG medium.

In a classical case Nd:YAG is analyzed as a four-level system (Fig. 2.5). Then relaxation of excitation takes four steps: I) Absorption of pump photon; II) fast relaxation to upper laser level while emitting a phonon; III) spontaneous or induced relaxation to lower laser level while emitting a photon; IV) fast relaxation to ground energy level, while emitting another phonon. Once Nd ion is in the ground energy level state, it can absorb a pump photon again.

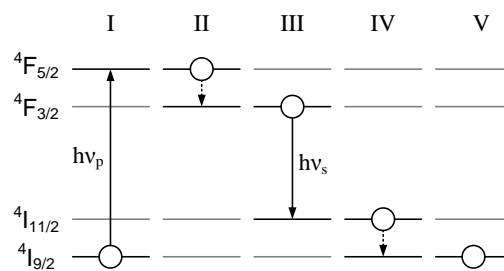


Fig. 2.5 Classical relaxation scheme of excitation in Nd:YAG.

Using such formalism it was derived from rate equations that heat generation in excited Nd doped medium is dependent on absorbed pump power only. The amount of generated heat versus absorbed pump power is equal to the difference of absorbed and emitted photons. This difference is often called a quantum defect.

When concentration of active ions is high, distances between ions is small and probability of interaction between them is higher. Interaction between active ions usually

comes up as non-radiative relaxation of excited ion. In Nd:YAG case, when doping concentration is high, at least two types of interactions have to be taken into account: upconversion and cross-relaxation (Fig. 2.6).

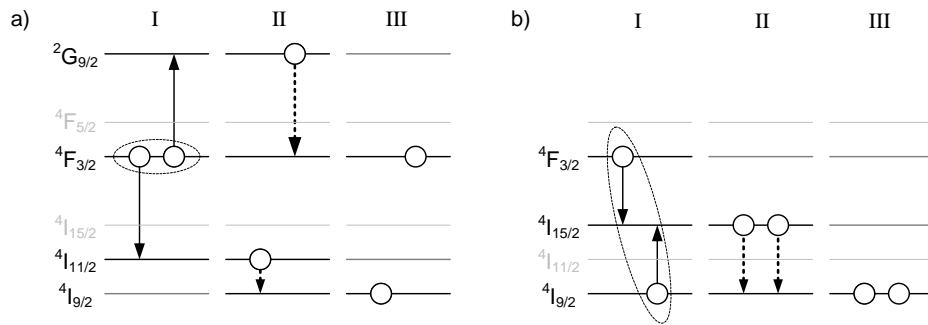


Fig. 2.6 Mechanisms of interaction between two active ions: a) upconversion; b) cross-relaxation.

Upconversion is occurring between two excited ions, when one of ions relaxes to lower energy level giving its energy to neighboring ion which is excited to higher energy level. Then first ion rapidly relaxes to ground level and other ion relaxes back to upper laser level. During this process energy of one excitation is converted to phonons which mean additional heat being generated (Fig. 2.6a). The rate of upconversion process in active laser medium is dependent on doping concentration and is proportional to population of excited ions squared [4,6-8]. This means that more excessive heat is generated as pump intensity is increased.

Cross-relaxation is occurring between two neighboring ions when one of them is in excited state and another is in ground state. Then part of energy of excited ion is transferred to un-excited ion and they both appear in intermediate energy level. Then both ions relaxes to ground state emitting phonons (Fig. 2.6b). Again, excessive heat is generated during this process. The rate of cross-relaxation also depends on doping concentration, but in this case it is proportional to the product of excited and un-excited ions populations [6,9-11].

There is one more type of non-radiative relaxation, when Nd^{3+} ion relax to ground state rather than to upper laser level when pump photon is absorbed. This mean, that ion does not participate in population inversion after absorbing a pump photon and all the energy is dissipated as phonons. The nature of such process is not thoroughly investigated, but it seems that it is related to the growing defects in crystals [10-12]. Anyway this effect can be included in rate equations as quantum efficiency of

absorption, which means that not all of absorbed pump photons create population inversion of laser medium.

All those effects are included in dissertation when rate equations are derived. Main result from these equations is that heat in Nd:YAG medium has four sources: due to quantum defect, due to upconversion, due to cross-relaxation and due to quantum efficiency.

In contrast to classical four-level system rate equations, heat fraction of absorbed pump power being generated in Nd:YAG medium is dependent on pump and amplified radiation intensities (Fig. 2.7).

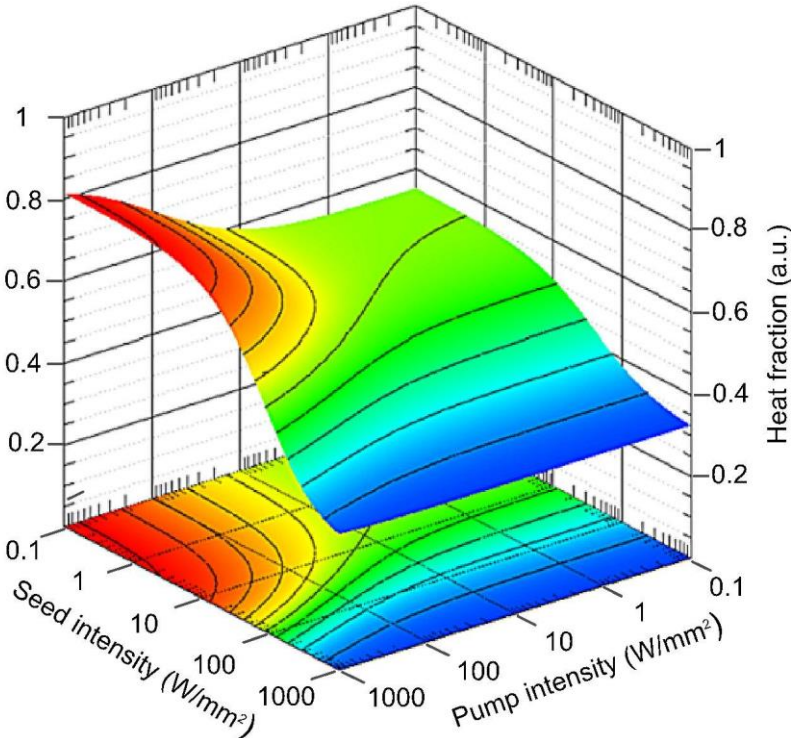


Fig. 2.7 Ratio between heat and absorbed powers dependence on pump and amplified radiation intensities for Nd:YAG with 2at.% doping .

2.4 Calculation of heat flows and deformations

In this work modeling of heat flows were performed using Comsol Multiphysics® software. This software allows calculating a temperature distribution in a defined model consisting of different materials and with different boundary conditions. After calculating the temperature distribution, stresses due to thermal expansion can also be calculated enabling evaluation of deformations of surfaces.

In general case parameters of medium (such as thermal conductivity, thermal expansion, Young's modulus, Poisson's ratio, etc.) are anisotropic and depend on temperature. It was assumed that materials are isotropic in this work.

When temperature changes in the medium are low, it can be assumed that thermo-mechanical properties of the medium are constant. Such approximation turns the problem into linear functions which are much easier to calculate and demands on computational resources are significantly lower.

In order to simplify the problem even more, another assumption was done that heat source in thin active layer is constant along z direction (over the thickness). Such assumption is valid when absorbing layer is thin and is widely used in literature [2,5,13]. Using this approximation enables to switch from three-dimensional computations to two-dimensional computations, thus saving computational resources even more.

In dissertation the use of linear approximations are analyzed in detail showing some specific issues of discrete computations to pay attention to. The main advantage of linear approximations is that finite element analysis software has to be used only once (for calculation of response functions of "delta" signal) and further calculations may be easily performed for various heat source distributions. This approach drastically reduces demands on computational resources.

2.5 Optical aberrations

As the laser beam propagates through medium where temperature is distributed unevenly, different parts of the beam travel different optical path due to refractive index variations caused by thermo-optic effect. Optical path also changes due to deformation of surfaces the beam passes or is reflected by. Optical path difference (OPD) for different parts of the beam changes phases of wave front resulting in distortions (aberrations). Aberrations affect the focusability (M^2 parameter) of a laser beam by worsening it in most cases. That is why it is important to evaluate laser element properties in respect of optical aberrations.

In dissertation the way to calculate OPD due to temperature distribution in the transparent medium and due to deformation of surfaces is described in more detail and useful formulas are derived.

2.6 Method for evaluation of aberrations

For evaluation of resulting wave front distortions, separation into spherical and aspherical parts of optical aberrations is typically performed [14] which is not very intuitive especially when applying to a Gaussian beam. It is also tricky to compare several different aberrated wave fronts when the amplitudes of distortions are similar but shapes are different.

We chose a different approach: to calculate a beam propagation parameter (M^2) of a Gaussian beam after reflection from a thin disk, acting as an aberrated mirror. Calculation of the M^2 parameter can be done numerically by simulating diffractive propagation using Fresnel integrals and calculating beam diameters at various distances (as it is performed in real M^2 measurement systems according to ISO 11146 standard).

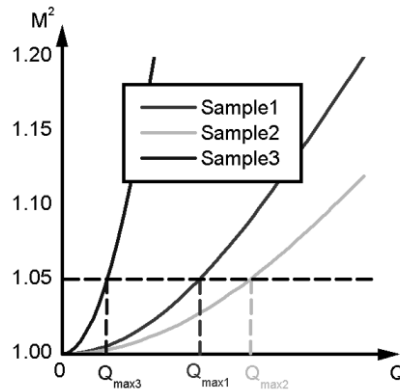


Fig. 2.8 Typical M^2 parameter dependence on the heat source density (pump power) of the reflected Gaussian beam from a thin-disk. Samples correspond to different geometries, heat source distributions or probing beam sizes.

Increasing the pump power to the thin-disk results in an increased amount of generated heat in the active medium, thus the heat source density (heat power per volume) increases. A higher heat source density results in stronger wave front aberrations of the reflected beam, which reduces the quality (brightness) of an affected Gaussian beam (Fig. 2.8).

We set a level of the acceptable M^2 parameter to be 1.05. Then we searched for the maximum heat source density Q_{max} fulfilling this condition (Fig. 2.8). This parameter indirectly represents capability of thin-disk geometry to manage a particular heat source, keeping aberrations under a certain level. In this way it is possible to compare different geometries of capped disks in the sense of thermal management. From the practical point

of view this Q_{max} parameter roughly represents the available output power from a laser oscillator or an amplifier with the predefined beam quality, as the output power is proportional to the absorbed pump power and part of the absorbed power is always converted to heat. It is important to note, that the Q_{max} parameter depends not only on geometry of thin-disk, but on the heat source distribution and the laser beam size on the disk as well. Adding undoped layer does not change absorption, amplification or heat generation properties in active volume, thus different geometries can be compared under the same conditions of the heat source and the probing beam. It is also worth to note that level of the acceptable M^2 parameter is not strict and different values may be chosen, resulting in different calculated Q_{max} parameters (Fig. 2.8).

2.7 Calculation of laser beam parameters

Derivation of methods to calculate a propagation of a coherent beam starts from scalar wave equations. Then it is shown that it is useful to exploit Fourier transformations in calculations as Fast Fourier Transform (FFT) can be used in discrete case. Basically, complex amplitude distribution of a beam at certain distance can be calculated in three steps which consist of Fourier transform, multiplication by a phase factor and inverse Fourier transform. Some issues caused by the properties of Fourier transform are also described in dissertation.

Most popular definition of M^2 parameter is that M^2 is a factor describing how much divergence of beam is bigger than that of an ideal Gaussian beam when the waist of the beam is the same. There are other definitions of the M^2 parameter which mean the same thing. But all of them are using a beam diameter which can be defined in many ways.

Siegman showed that for M^2 parameter calculations a proper way to define a beam diameter is by second moment width [16]. Then practically any beam follows a hyperbolic function of beam diameter along its propagation direction:

$$\omega^2(z) = \omega_0^2 + (M^2)^2 \left(\frac{\lambda}{\pi\omega_0} \right)^2 (z - z_0)^2 . \quad (2.5)$$

Meanwhile using other definitions of beam diameter are not applicable in M^2 parameter calculations in most cases.

The calculation principles of beam diameter by second moments are defined by ISO11146 standard. This standard is used to derive methods of beam diameter calculations in discrete case, which is analyzed in more details in the dissertation.

As it can be seen from (2.5), M^2 parameter can be calculated by following equation:

$$M^2 = \frac{\pi\omega_0\sqrt{\omega^2(z)-\omega_0^2}}{\lambda(z-z_0)}. \quad (2.6)$$

Thus, in order to calculate M^2 parameter we need to know the beam diameter at the waist and at some distance from the waist.

As calculation of beam diameter at certain distance (by calculation of beam propagation) requires quite some computational resources, a search for a beam waist should take as few steps as possible. A specialized efficient algorithm to find the position of the waist is presented in dissertation which usually gives enough data to calculate the M^2 parameter also.

3 Experiments

3.1 Composite element

Characterization of pump

An interesting result was noticed when a formed pump beam was characterized: intensity distribution is not symmetric in respect of waist plane as the beam propagates (Fig. 3.1).

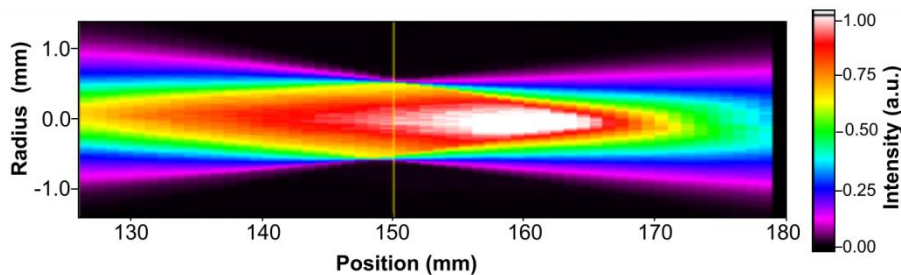


Fig. 3.1 Intensity distribution variations as the pump beam propagates after pump formation optical system.

In order to understand reasons for such behavior of pump beam, a simple model was developed (see chapter 2.2) and then confirmed (chapter 3.2) showing a good agreement to experimentally measured data.

Generation and amplification

Optical scheme for generation experiments is shown in Fig. 3.2. Reflectivity of output coupler of the plane resonator was 95%. Such resonator generates multimode laser beam. Output power dependence on absorbed pump power is shown in Fig. 3.2. It showed a good slope efficiency of 40% when generation threshold is 7W. Nevertheless, efficient generation of single transversal mode could not be obtained. Depending on resonator configuration, maximum power of a diffraction limited beam was either 2.5W (at 60W absorbed pump power) or 1.8W (at 20W absorbed pump power). With enhanced thermal interface it was possible to obtain somewhat higher power in single-mode regime, which was 4.2W. It was obvious that induced aberrations are much higher than it was expected from early-stage numerical simulations.

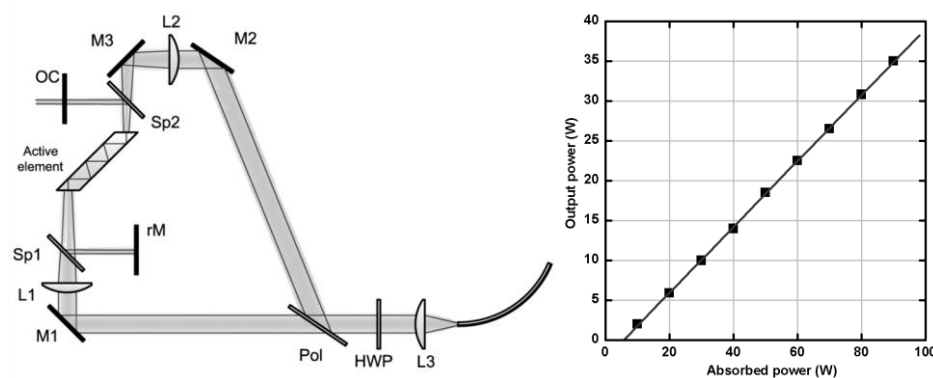


Fig. 3.2 Optical scheme for generation measurements of composite active element and output power dependence on absorbed pump power

This means, that numerical model has to be modified. Simplified model was checked by indirect temperature measurements using generation wavelength dependence on temperature. Estimated “average” temperature rise in active zones were about 45K.

The presence of strong aberrations was also evident after measuring characteristics of an amplified laser beam from external source with a diffraction limited beam. Power amplification properties did not show any unexpected results as well as generation in multimodal regime. But characterization of amplified beams showed that aberrations are already detrimental even when seed beam is almost twice smaller in diameter compared to pump beam at its waist (Fig. 3.3).

The composite element also showed strong thermal-lensing effect, as the amplified beam was focused at about 80 mm distance after passing the laser element. For this reason, characteristics of beam propagation were measured by shaping it with two

lenses: one to collimate the beam and another to focus it in order to have a waist in the CCD camera movement range.

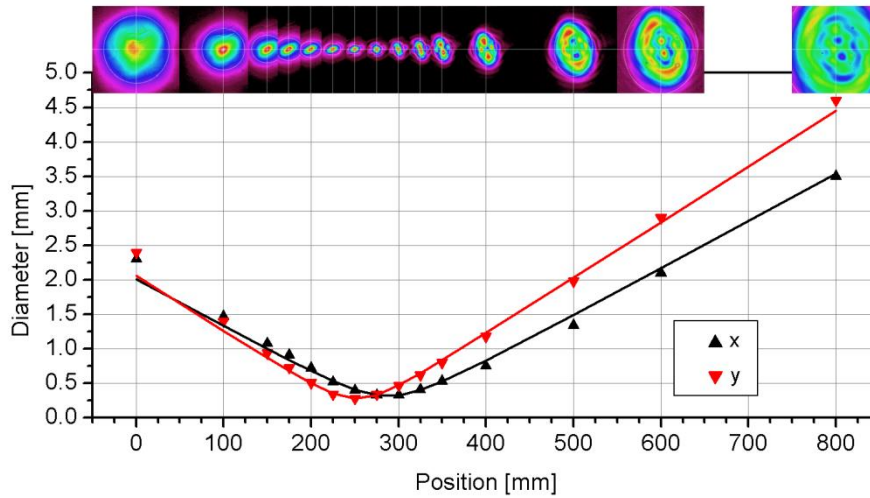


Fig. 3.3 Propagation of an amplified beam, when seed beam diameter is 0.65mm FWHM.

Measurements of aberrations

Aberrations induced in the composite element were measured by Mach-Zehnder interferometer based on He-Ne laser. After analyzing interferograms, results showed the manner of aberrations (Fig. 3.4). It can be seen that there is a strong thermal lens with aberrations including astigmatism.

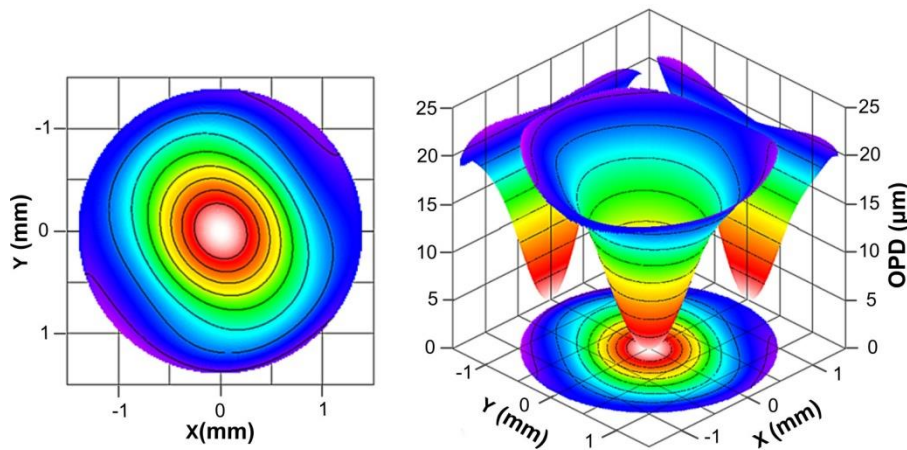


Fig. 3.4 OPD obtained from interferograms at maximum pump power (100 W).

According to symmetry rules, astigmatism should be oriented either on x or y axis, but it is rotated in experiments. This can be explained by the fact that experimental setup was not completely symmetrical as beams were propagating closer to one side of the sample.

Summary of experimental results

A composite sample showed good absorption and multimode generation properties. Nevertheless, strong thermally induced aberrations did not allow obtaining an effective diffraction limited beam generation. Strong thermal lens and aberrations were not expected due to similarity to thin-disk laser elements

3.2 Experimental validation of theoretical models

Pump beam propagation

Pump beam propagation model was confirmed using experimental data from pump beam characterization measurements and theoretical model from section 2.2. Results show a good agreement between calculated (Fig. 3.5) and experimental (Fig. 3.1) data.

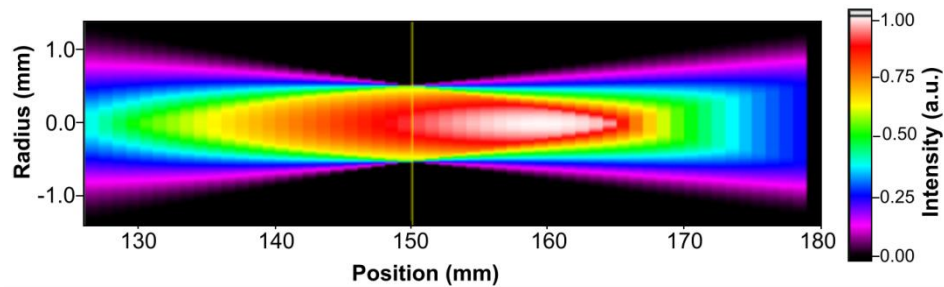


Fig. 3.5 Pump beam intensity distribution variation over distance comparison as it propagates (numerical simulation).

More details on modeling parameters are presented in dissertation.

Absorption of Nd:YAG

A sample made of composite Nd:YAG/YAG ceramics was prepared. The sample size was 8x8x1.2 mm with the 0.2 mm thickness layer doped with Nd^{3+} of 2 at.% concentration. The surface on the doped side was highly reflective for 808 nm and 1064 nm wavelengths, and the undoped side was antireflection coated (Fig. 3.6).

The sample was pumped by the fiber coupled laser diode emitting up to 100W @ 808nm. The pump spot was formed by the magnified image relay of the fiber end. The pump spot diameter on sample was 2.2 mm. A short multimode resonator was also formed to measure non-saturated absorption also (Fig. 3.6).

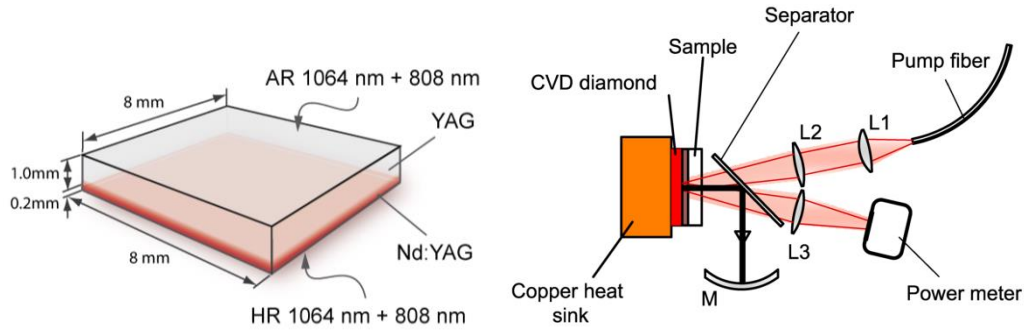


Fig. 3.6 Geometry of sample used for experiments and experimental setup for absorption measurements.

According to the rate equations derived in section 2.3, absorption should be saturating resulting in different absorption under lasing and non-lasing conditions. This is evident from Fig. 3.7 where experimental data show a good agreement to theoretical data. An effective absorption cross-section varies due to changing spectrum of pump radiation of laser diode.

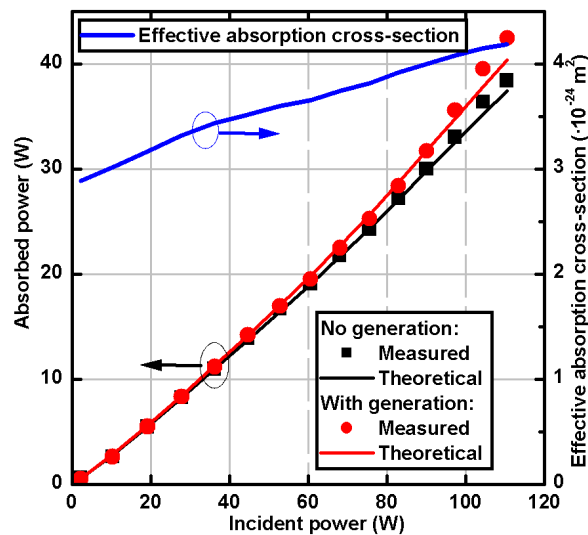


Fig. 3.7 Measured and theoretically calculated absorbed power dependence on incident pump power.

Thermally induced optical aberrations

For measurements of thermally induced optical aberrations experimental setup with probe beam from single mode fiber and Shack-Hartmann wavefront sensor was used (Fig. 3.8). The sample was attached to the 8x8x0.5 mm CVD diamond plate and a water cooled copper plate. Bonding layers were “Antec Formula 7” thermal compound with the measured thicknesses of 25 μm . Besides good thermal conductivity of compound (8 W/m·K), heat resistance of the layer was estimated to be about 5 W/(cm²·K).

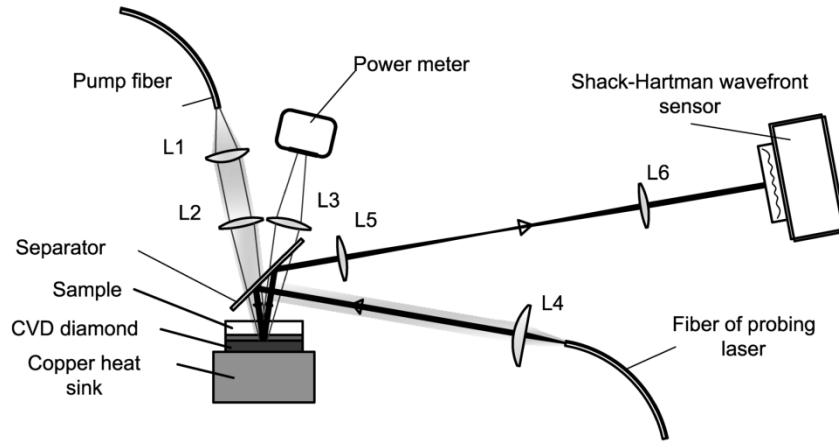


Fig. 3.8 Experimental setup for measurements of aberrations.

The sample was pumped by the fiber coupled laser diode emitting up to 100W @ 808nm. The pump spot diameter on sample was 2.2 mm. The collimated output of the single-mode fiber coupled laser diode emitting at 1064 nm was used for probing. Induced wave front changes were measured by relaying the sample image plane to the Shack-Hartmann wave front sensor using a 4F telescope (Fig. 3.8).

The dissipated heat power had to be estimated to compare experimental data with results of numerical modeling. This was done by solving steady state rate equations including cross-relaxation and upconversion effects (section 2.3). High levels of population of inversion were expected, which was manifested by good agreement of calculated and measured saturated pump absorption in the sample. High inversion levels in the Nd^{3+} doped medium give excessive conversion of the absorbed laser diode power to the heat power (it was estimated to reach 70% in our case).

The estimated maximum heat source density was about 30 W/mm³. With such a heat source power a nearly 200K maximum temperature rise in the sample was expected (Fig. 3.9), and nonlinear effects (dependence of heat conductivity and expansion coefficient on temperature) had to be taken into account. This is evident from comparison of experimental data with calculated values of OPD using linear approximation. The linear approximation resulted in reduced variation of OPD over radius and a different shape of OPD distribution (apex is less sharp) (Fig. 3.10a). Experimentally measured variation of OPD over radius (span between the minimum and maximum OPD value) also manifests non-linear dependence on the heat power (Fig. 3.10b).

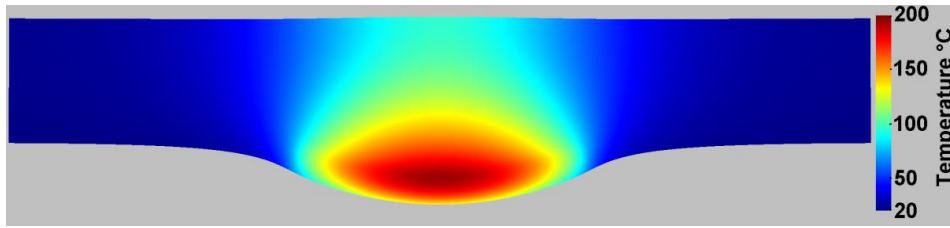


Fig. 3.9 Calculated temperature distribution and deformation of surfaces (magnified 500 times) under maximum pump conditions.

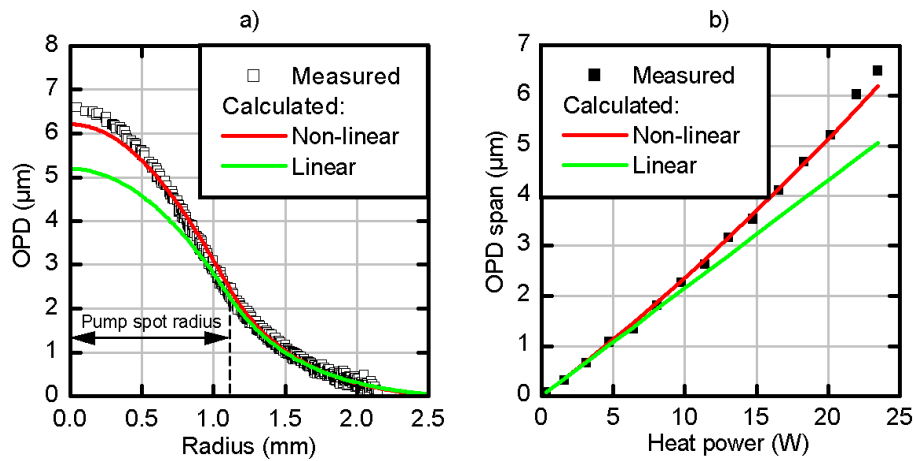


Fig. 3.10 Comparison of experimental and calculated data: a) measured OPD under maximum pump conditions and calculated OPD in linear and non-linear approximations; b) OPD span (minimum to maximum OPD value difference) dependence on the dissipated heat power.

Concluding these results, measurements showed that developed models gives results that are close to experimental data and can be used for calculations.

Calculation of laser beam propagation

For verification of beam propagation calculations, experimental data was also used. Data obtained from measurements of wave front aberrations was used. Those aberrations were applied to ideal Gaussian beam and propagation properties of this affected beam were calculated. Results of calculations were compared with measured beam intensity profiles from experiments, showing a very good agreement between measured and modeled data.

These results confirmed that beam propagation is being calculated correctly, and evinced on the quality of analysis of interferograms obtained during measurements of aberrations.

4 Theoretical estimation of optical properties of composite active elements

In order to understand the source of induced aberrations seen in experiments, composite element was simplified to a single thin disk with an undoped layer on top (Fig. 4.1).

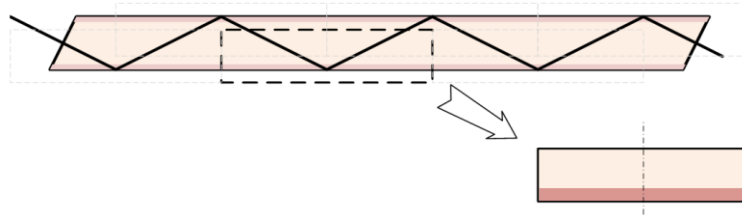


Fig. 4.1 Simplification of a composite element to a thin disk with an undoped layer on top.

Adding an undoped layer on the thin-disk changes temperature distribution inside the structure and character of deformations (Fig. 4.2). Mounting technology is also important as some deformations (such as flexing of the thin-disk) may be suppressed (Fig. 4.2c and Fig. 4.2d).

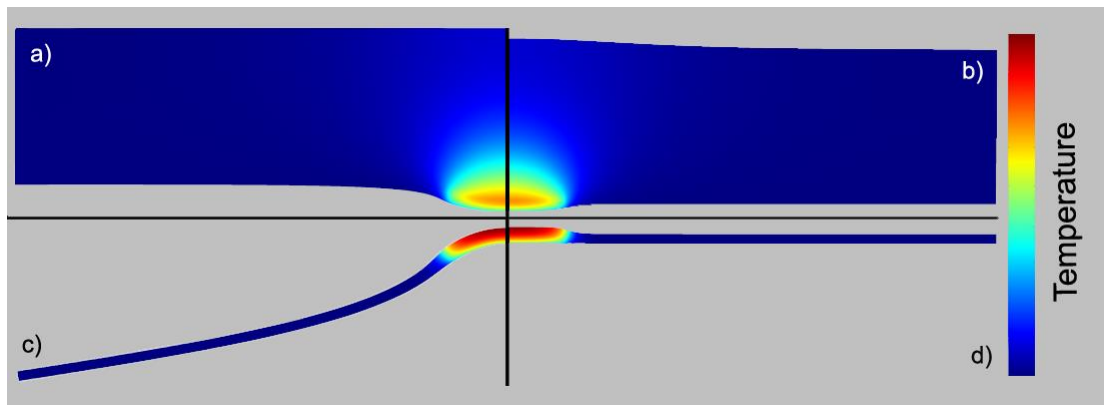


Fig. 4.2 Calculated temperature distribution and deformations of surfaces (magnified 2000 times) of a thin-disk with a thick undoped layer (a and b) and an uncapped disk (c and d) with unconstrained deformations (a and c) and deformations suppressed by indium solder (b and d). Heat source distribution (pumping conditions) is the same for all cases.

As the previous numerical model gave results consistent with experimental data, this thermo-mechanical model of the thin-disk was used for evaluation of the influence of the undoped layer thickness on resulting optical aberrations.

All further calculations were performed in linear approximation, meaning that heat conductivity and thermal expansion coefficients were set to be temperature-independent.

Motivation for the linear approximation is mainly related to computer resources. Despite the fact that linear approximation does not allow an accurate evaluation of wave fronts or the beam quality, it still gives sense on the influence of various sample and pump/probe parameters such as the thickness of the undoped layer, the size of the pumped region or mode overlap (fill factor). Meanwhile the calculation time may be reduced drastically.

4.1 Model geometry

Numerical modeling was performed using the finite-element analysis using COMSOL Multiphysics[®] software. Model geometry was set to have radial symmetry, disk radius was set to be 20 mm which is large enough to consider an infinitely large disk as increasing radius further has no significant effect on the modeling results within the scope of pump and probe beam parameters being analyzed. Doped and undoped regions were not separated as different materials. A heat source was bounded by the pump radius (R_p) and the doped layer thickness (d) (Fig. 4.3). Two cases of boundary between the crystal and cooling plate were modeled. In the first case we set a heat transfer coefficient to be $h=10\text{W}/(\text{cm}^2\cdot\text{K})$ to a heat-sink with temperature $T_0 = 20^\circ\text{C}$ and let this surface to deform freely (Fig. 4.3a). Such situation corresponds to direct water cooling or thermal grease as a bonding layer. In another case an additional indium layer ($d_{\text{In}}=100\mu\text{m}$) was introduced. The opposite surface of indium layer was set to have constant temperature ($T_0 = 20^\circ\text{C}$) and was mechanically fixed. In this way deformation of the disk was partially suppressed (Fig. 4.3b), corresponding to soldering a thin disk to a stiff heat sink. The boundary between the crystal and indium was set to have heat resistance with a heat transfer coefficient chosen in the way that the efficient heat transfer coefficient was the same as in the previous case. All other surfaces were thermally insulated in both cases.

The thickness of the doped (active) layer was $d = 0.2$ mm (Fig. Fig. 4.3) for all cases. The thickness of the undoped layer was altered by setting the overall structure thickness (D in Fig. Fig. 4.3), thus 0.2 mm represents the uncapped thin-disk. The thickness was increased by the factor of 2 up to 3.2 mm (0.2 mm, 0.4 mm, 0.8 mm, 1.6 mm and 3.2 mm).

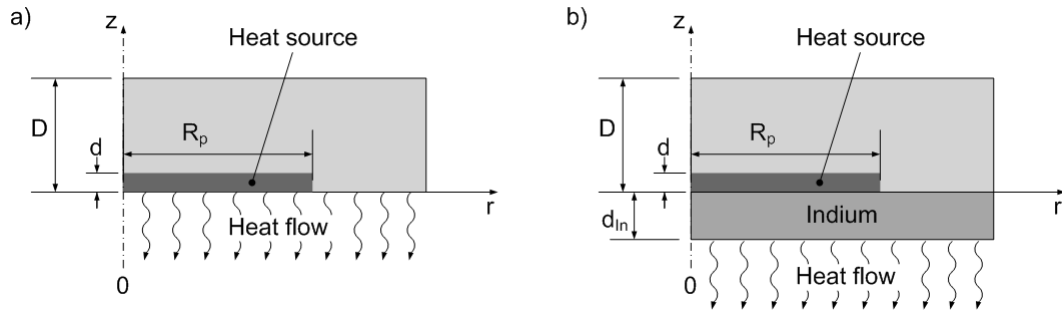


Fig. 4.3 Model geometry used in numerical calculations: a) freely deformable; b) constrained by indium layer.

Two types of heat source density distributions over pump spot radius were modeled: hat-top (cylindrical) and Gaussian. A size of Gaussian distribution is defined as the diameter at $1/e^2$ level. A size of hat-top distribution is defined as the diameter of boundaries. Heat source distribution in z direction was constant, bounded by the doped layer thickness. It is worth noting that at such definitions of heat source sizes the total heat power of hat-top distribution is two times higher than that of Gaussian distribution if the maximum value of the heat source density is fixed the same.

4.2 Evaluation of influence of undoped layer

In the first computer modeling run, the laser beam size was fixed to be 2 mm. The maximum heat source density dependence on the heat source size for which M^2 of the reflected laser beam was less than 1.05 (Q_{max} parameter), is presented in Fig. 4.4. A general tendency is that by increasing the heat source (pump) size, while keeping the laser beam size fixed, samples of all modeled thicknesses can operate with a good beam quality at higher heat loads. The larger pump size, the larger the heat load is acceptable for a good beam quality. This could be expected as temperature and deformations are distributed more evenly over an effective area of the laser beam. But it comes at the cost of efficiency as the pumped area (thus required pump power) is a function of the transverse size squared. Another drawback of an increasing pump spot size is that ASE also increases and a thicker undoped layer is needed [1], which in most cases has detrimental effects on optical aberrations. A substantially larger pump spot size than that of the laser beam size demands special care in designing laser resonators to suppress higher order resonator modes (hard apertures have to be introduced) [5].

An interesting region for freely deformable disk is when the size of the heat source with Gaussian distribution is similar to the laser beam size (Fig. 4.4c). Theoretically it seems to be the region where the efficiency in conjunction with a good beam quality may be achieved as flexing of the disk is partially compensating aberrations due to the refractive index change and smaller scale surface deformations. But from the practical point of view this region is unstable as it highly depends on the heat source distribution (Fig. 4.4a and Fig. 4.4c). It also depends on the size of the laser beam which can be seen by comparing Fig. 4.4c with Fig. 4.5c where the same plot is presented for the laser beam size of 4 mm. Here (Fig. 4.5c) the uncapped freely deformable thin disk becomes the worst case scenario and a thin-disk with the overall thickness of 0.4 mm becomes favorable.

When flexing of the disk is partially suppressed (in our case by indium solder, assuming that other surface of indium is mechanically fixed), results become more predictable and controllable which is desired in realistic applications (Fig. 4.4b and Fig. 4.4d). Anyway, it is obvious that adding an undoped layer on a thin disk has detrimental effects in respect of optical aberrations as higher heat loads (higher pump powers) can be managed by a thin-disk without or with a thinner undoped layer. In other words, adding an anti-ASE cap worsens the beam quality at the same heat load.

There are some effects emphasized by undoped layer which are not affecting the M^2 parameter but might be important to note in practical applications. One of undesirable effects of a thick undoped layer is thermal lensing. When a thick undoped layer is applied, deformation of each surface and temperature distribution in the medium mutually acts as a positive lens (illustrated in Fig. 3.9). Meanwhile flexing of uncapped (or with thin undoped layer) disk tends to form a convex mirror which may compensate or even overcome positive lens due to temperature distribution and bulging of the disk (Fig. 4.2). Another detrimental effect of a thick undoped layer observed during experiments is depolarization. This effect was not thoroughly analyzed, but could be explained by induced radial stresses due to an emerging radial heat flow, which is usually kept low in the uncapped thin-disk case.

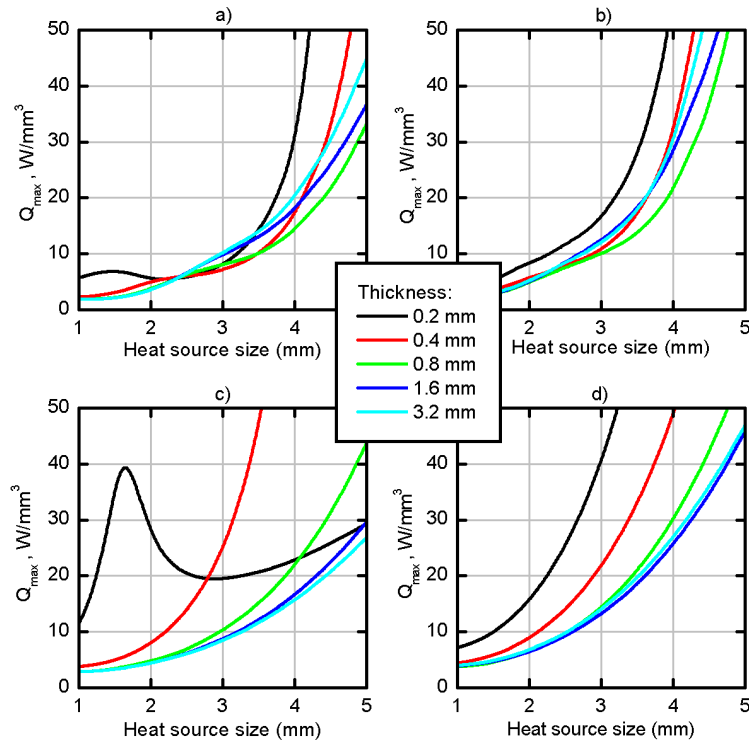


Fig. 4.4 Dependence of Q_{max} parameter on the heat source size for 2 mm laser beam size: a) and c) freely deformable geometry; b) and d) geometry with indium solder; a) and b) hat-top heat source; c) and d) Gaussian heat source.

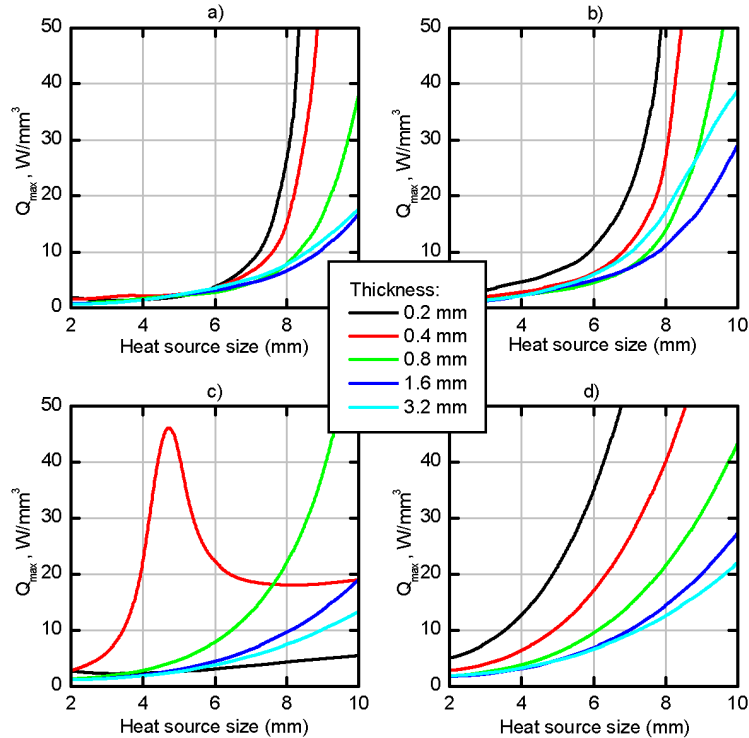


Fig. 4.5 Dependence of Q_{max} parameter on the heat source size for the 4 mm laser beam size: a) and c) freely deformable geometry; b) and d) geometry with indium solder; a) and b) hat-top heat source; c) and d) Gaussian heat source.

According to [16] the scaling procedure is as follows: for doubling the output power, double the pump power and the mode area on the disk, while keeping the disk thickness and the output coupler transmission constant. This defines that the pump intensity (thus the heat source density) is kept constant and the pump spot (heat source) size is mutually increased with the laser beam size.

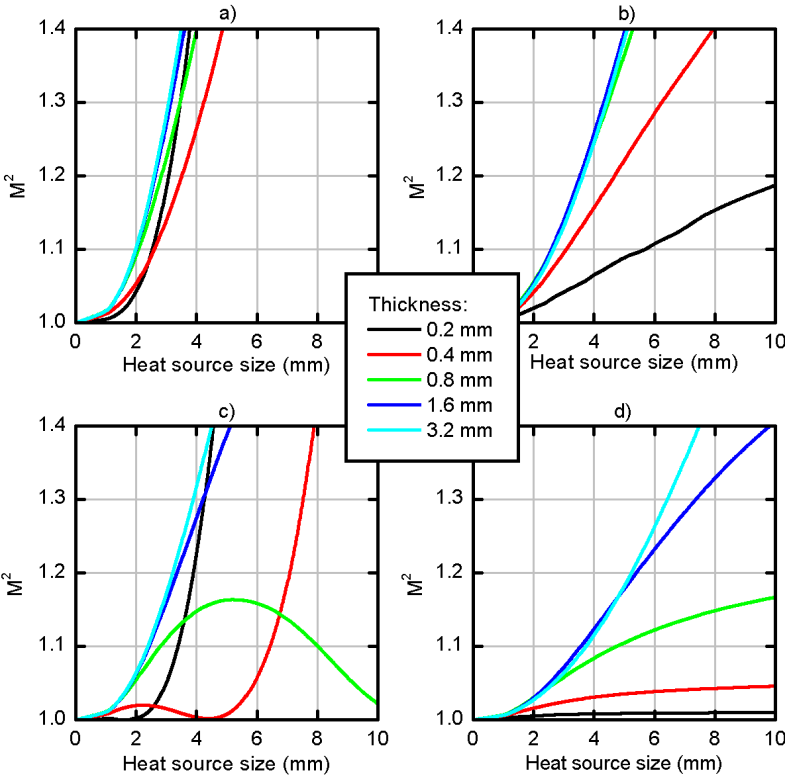


Fig. 4.6 Dependence of M^2 parameter on the heat source and the laser beam size (fill factor 1): a) and c) freely deformable geometry; b) and d) geometry with indium solder; a) and b) hat-top heat source; c) and d) Gaussian heat source.

For estimation of the power scalability the heat source density was fixed at $Q = 5 \text{ W/mm}^3$ and the M^2 parameter dependence on the heat source size was plotted (Fig. 4.6). The laser beam size was kept the same as the heat source size (fill factor 1). According to the data in Fig. 4.6, scaling is limited by degradation of the reflected laser beam quality. Generally, the M^2 parameter is increasing as the sizes of the heat source and the laser beam are mutually increased. Moreover, freely deformable disks show some regions of low aberrations but demand a certain distribution of heat source (Fig. 4.6c). When deformations are suppressed by indium solder, the beam quality can be improved (or the pump power can be increased). A further improvement may be achieved by switching from the hat-top heat source (pump) distribution to the Gaussian

one. The Gaussian distribution of the pump intensity is also desirable in fundamental mode laser resonators as it helps to maintain a fundamental mode. In case of the heat source with the Gaussian distribution the uncapped or thin disk with a thin undoped layer seems to satisfy the power scalability concept as an increase of the M^2 parameter tends to saturate as sizes of the pump and laser beam are increasing (Fig. 4.6d). Nevertheless, increasing of the thickness of the undoped layer diminishes this effect (Fig. 4.6d).

As mentioned earlier, by sacrificing efficiency, the increasing heat source (pump) size in respect of the laser beam size improves the reflected laser beam quality (or higher power levels may be achieved). Nevertheless, characteristics of the M^2 parameter over scaling remain similar to those presented in Fig. 4.6.

To this point only a normal incidence angle of beams was analyzed. Nevertheless, in dissertation it is shown that for thick undoped layer case changing the angle of incidence of beams does not change the manner of aberrations significantly, just some degree of astigmatism is introduced.

4.3 Estimations for alternative multi-disk configuration

As the main source of thermally induced aberrations in the composite laser active element arise from the presence of undoped medium, it would be logical to avoid it. This would mean to go back to the multi-disk concept which is based on separate thin-disk laser elements (Fig. 1.1). It could be a further way to investigate the proposed multi-disk concept.

Main advantages of the configuration of separate thin-disks to monolithic design would be already mentioned thermal management and ability to optimize heat power distribution between individual disks by altering either thickness or doping concentration. But one has to keep in mind, that total internal reflection could not be used anymore, requirements on pump beam would be higher and there is a risk that amplified spontaneous emission may become a limiting factor.

Conclusions

- A concept of composite laser element with thin active layer was introduced. This concept combines properties of several types of laser active elements: shape of the element is similar to slab type laser elements; end-pumping scheme is usually used for rod type laser elements; thermal management is similar to thin-disk laser elements. Such kind of laser element is possible to realize due to transparent ceramic material manufacturing technologies which allow to make a laser element of desired shape and composition (in the sense of doping).
- Experimental results show, that proposed laser element attributes to have high thermally induced aberration despite its similarity to thin-disk laser element. From this point of view this element has no advantage over common rod type laser element.
- A method to rate different optical phase distortions induced by optical elements based on calculations of resulting M^2 parameter of an affected diffraction limited laser beam was proposed. This method enabled to estimate the influence of undoped layer on top of thin active layer. Results show that adding undoped layer deteriorates propagation properties of the reflected diffraction limited laser beam.
- Wave front aberrations arise mostly due to edge effects which can be reduced by using pump beams with Gaussian intensity profiles. Other way for reduction of aberrations is to increase the size ratio of pump and laser beams, but one has to keep in mind that power efficiency will be reduced.
- Analysis of simplified numerical models showed that main reason for aberrations in proposed active element is the undoped medium between thin active layers. Regardless of advantages of monolithic structure, withdrawal of undoped filling between thin active layers should provide lower optical aberration maintaining similar absorption and amplification properties. In case of mastering a thin-disk bonding to a heat sink technology it could be a further way to investigate the proposed multi-disk concept.
- Generally, a pump beam is asymmetric in respect of its waist plane when it is formed by optical system after out-coupling from a large core diameter fiber. This can be important when laser element is relatively long. A simple model to calculate the variation of intensity distribution as the beam propagates after passing optical system was presented.

References

- [1] D. Kouznetsov, Role of undoped cap in the scaling of thin-disk lasers, *J. Opt. Soc. Am. B* **25**, 338–345 (2008).
- [2] D. Bossert, P. Avizonis, and A. Killi, Comparative performance of ASE suppressed ceramic Yb:YAG thin disks, in *Proc. SPIE 7578*, vol. 7578, W. A. Clarkson, N. Hodgson, and R. K. Shori, eds., 75780G (2010).
- [3] M. M. Tilleman, Analysis of thermal effects in laser materials, 2: Disk and slab geometry, *Optical Materials* **33**, 363–374 (2011).
- [4] V. Lupei, Ceramic laser materials and the prospect for high power lasers, *Optical Materials* **31**, 701–706 (2009).
- [5] A. Kemp, G. Valentine, and D. Burns, Progress towards high-power, high-brightness neodymium-based thin-disk lasers, *Progress in Quantum Electronics* **28**, 305–344 (2004).
- [6] M. Pollnau, P. Hardman, M. Kern, W. Clarkson, and D. Hanna, Upconversion-induced heat generation and thermal lensing in Nd:YLF and Nd:YAG, *Physical Review B* **58**, 16076–16092 (1998).
- [7] S. Guy, C. Bonner, D. Shepherd, D. Hanna, A. Tropper, and B. Ferrand, High-inversion densities in Nd:YAG-upconversion and bleaching, *IEEE Journal of Quantum Electronics* **34**, 900–909 (1998).
- [8] Y. Chen, C. Liao, Y. Lan, and S. Wang, Determination of the Auger upconversion rate in fiber-coupled diode end-pumped Nd:YAG and Nd:YVO₄ crystals, *Applied Physics B: Lasers and Optics* **70**, 487–490 (2000).
- [9] H. G. Danielmeyer and P. Balmer, Fluorescence Quenching in Nd:YAG, *Applied Physics* **274**, 269–274 (1973).
- [10] D. C. Brown, Power Densities and Fractions in Nd:YAG, *IEEE Journal of Quantum Electronics* **34**, 560–572 (1998).
- [11] T. Fan, Heat generation in Nd:YAG and Yb:YAG, *IEEE Journal of Quantum Electronics* **29**, 1457–1459 (1993).
- [12] D. P. Devor, L. G. DeShazer, and R. C. Pastor, Nd:YAG quantum efficiency and related radiative properties, *Quantum Electronics, IEEE Journal of* **25**, 1863–1873 (1989).

- [13] K. Contag, M. Karszewski, and C. Stewen, Theoretical modelling and experimental investigations of the diode-pumped thin-disk Yb: YAG laser, *Quantum Electronics* **29**, 697–703 (1999).
- [14] J. Mende, E. Schmid, J. Speiser, G. Spindler, and A. Giesen, Thin-disk laser - Power scaling to the kW regime in fundamental mode operation, in *Proc. SPIE 71931*, , W. A. Clarkson, N. Hodgson, and R. K. Shori, eds., V1–12 (2009).
- [15] A. E. Siegman, How to (Maybe) Measure Laser Beam Quality, *DPSS (Diode Pumped Solid State) Lasers: Applications and Issues*, vol. 17, M. W. Dowley, ed. (Optical Society of America, 1998), 184–199 (1998).
- [16] R. Paschotta, Power scalability as a precise concept for the evaluation of laser architectures, *2007 European Conference on Lasers and Electro-Optics and the International Quantum Electronics Conference*, (2007).

Santrauka

Disertacijos darbo tikslas buvo, modeliuojant bei vykdant eksperimentus, išanalizuoti siūlomo sudėtinio aktyvaus lazerio elemento koncepcijos prielaidas ir taikymų galimybes, bei surasti veiksnius, ribojančius pasiūlyto sudėtinio aktyvaus lazerio elemento galimybes.

Šiame darbe buvo pasiūlytas lazerio aktyvusis elementas, kuris apjungia įvairių tipų lazerinių aktyviųjų elementų gerąsias savybes. Tačiau eksperimentai parodė, jog toks sudėtinis elementas neturi pranašumo prieš plačiai naudojamus strypo formos lazerinius aktyvius elementus.

Siekiant paaiškinti susidarančių optinių iškraipymų priežastis, buvo sukurti ir pritaikyti teoriniai modeliai, aprašantys aktyvios terpės optines, termo-optines bei termomechanines savybes. Sukurtas optinių iškraipymų vertinimo metodas, leidžiantis palyginti skirtingų konfigūracijų elementus šiluminių reiškinių sąlygotų optinių iškraipymų atžvilgiu. Taip pat pateiktas paprastas modelis, gerai aprašantis iš daugiamodžio šviesolaidžio išėjusios kaupinimo spinduliuotės intensyvumo skirstinio kitimą. Visi pateikti teoriniai modeliai buvo patvirtinti eksperimentiniais matavimais.

Naudojantis sukurtais teoriniais modeliais buvo nustatyta, jog pagrindinė optinių iškraipymų priežastis siūlomame sudėtiname lazeriniame elemente yra nelegiruota terpė tarp plonų legiruotų sluoksnių, kurioje vykstantys šiluminiai reiškiniai riboja tokio lazerinio aktyvaus elemento galimybes.

Siūloma tolimesnė pateiktos koncepcijos vystymo kryptis yra nelegiruotos terpės atsisakymas, taip gaunant atskirų plonų diskelių daugiadiskinį lazerinį aktyvųjį elementą.

Brief information about the author

Name: Aidas
Surname: Aleknavičius
Date of birth: March 7, 1984
Place of birth: Šilutė, Lithuania
e-mail: a.aleknavicius@ekspla.com

Education:

2002: finished Šilutės 1st gymnasium
2002-2006: bachelor studies at Faculty of Physics, Vilnius University. Study programme: Computer physics
2006-2008: master studies at Faculty of Physics, Vilnius University. Study programme: Laser physics and technology
2008-2012: PhD studies at Center for Physical Sciences and Technology; Vilnius University. Technological sciences.

Positions:

2005-2006: Technician at Institute of Material Science and Applied Research of Vilnius University, Picosecond photonics department.
2006- : Engineer at UAB “Ekspla”.
2008- : Engineer and junior research assistant at the Center for Physical Sciences and Technology.